

## ORIGINAL ARTICLE

Special Section: Tribute to Rien van Genuchten, Recipient of the 2023 Wolf Prize for Agriculture

# Unsaturated hydraulic property measurements of subtropical anthropogenic (purple) soils in China

Luwen Zhuang<sup>1</sup>  | Hao Chen<sup>1</sup> | Ping Yan<sup>2</sup> | Xingmei Liang<sup>1</sup> |  
Wenceslau G. Teixeira<sup>3</sup>  | Martinus Th. van Genuchten<sup>4,5</sup>  | Kairong Lin<sup>1</sup> <sup>1</sup>Center for Water Resources and Environment, and Guangdong Key Laboratory of Marine Civil Engineering, School of Civil Engineering, Sun Yat-sen University, Guangzhou, China<sup>2</sup>Guangdong Open Laboratory of Geospatial Information Technology and Application, Guangzhou Institute of Geography, Guangdong Academy of Sciences, Guangzhou, China<sup>3</sup>Soil Physics, Embrapa Soils, Rio de Janeiro, Brazil<sup>4</sup>Department of Earth Sciences, Utrecht University, Utrecht, The Netherlands<sup>5</sup>Department of Nuclear Engineering, Federal University of Rio de Janeiro, Rio De Janeiro, Brazil**Correspondence**Kairong Lin, Center for Water Resources and Environment, and Guangdong Key Laboratory of Marine Civil Engineering, School of Civil Engineering, Sun Yat-sen University, Guangzhou 510275, China.  
Email: [linkr@mail.sysu.edu.cn](mailto:linkr@mail.sysu.edu.cn)

Assigned to Associate Editor Céline Pallud.

**Funding information**

National Key Research and Development Program of China, Grant/Award Number: 2022YFC3002903; National Natural Science Foundation of China, Grant/Award Numbers: 42007165, 42377057

**Abstract**

Many anthropogenic soils, often referred to as red bed or purple soils, are distributed in various areas of southern China. Purple soils typically are highly weathered and often lead to natural and engineering hazards because of their relatively poor water retention properties. Knowledge of the unsaturated soil hydraulic properties of purple soils is crucial for their optimal management and various assessment studies. In this work, the hydraulic properties of purple soils from southern China were measured in the laboratory over the full moisture range using a combination of evaporation (HYPROP) and psychrometer (WP4C) approaches. Measured data were analyzed in terms of four different unimodal and bimodal soil hydraulic models. The measurements and analyses showed that bimodality was not overly significant for most samples. The good fit of the Peters–Durner–Iden models furthermore suggested that corner and film flows were important under relative dry conditions. Existing soil pedotransfer functions were found to provide a fairly close match for the slope of water retention curves with the exception of near saturated water contents and the saturated conductivity. To the best of our knowledge, this is the first time that unsaturated hydraulic data of purple soils are provided over the full moisture range.

## 1 | INTRODUCTION

Purple soils in the Soil Genetic Classification of China are lithologic soils developed from purple sedimentary rocks by weathering and erosion (Zhong et al., 2019). They are mostly

**Abbreviations:** BiVG, bimodal van Genuchten; BiVGPDI, bimodal van Genuchten–Peters–Durner–Iden; VG, van Genuchten; VGPDI, van Genuchten–Peters–Durner–Iden.

This is an open access article under the terms of the [Creative Commons Attribution-NonCommercial-NoDerivs](https://creativecommons.org/licenses/by-nc-nd/4.0/) License, which permits use and distribution in any medium, provided the original work is properly cited, the use is non-commercial and no modifications or adaptations are made.

© 2024 The Authors. *Vadose Zone Journal* published by Wiley Periodicals LLC on behalf of Soil Science Society of America.

classified as Regosols in the Food and Agriculture Organization taxonomy system (FAO, 1988) and as Entisols in the United States Department of Agriculture taxonomy system (He, 2003; Wei et al., 2006; Soil Survey Staff, 2022). Geologically, purple sedimentary rocks originated from “red beds,” which refers to red-colored sedimentary strata, including sandstone, mudstone, and shale, formed during different geological periods (Meng et al., 2023; L. Yan et al., 2019). For this reason, purple soils are also known as red bed soils (Turner, 1978), although the term “red bed” is used only minimally in the US soils and hydrology literature. Red beds are spread all over the world, especially in tropical and subtropical areas (X. C. Zhang et al., 2017; Zhou et al., 2019), including the humid areas of southern China (L. B. Yan & Milica, 2019). Purple soils, owing to their high fertility, hold significant importance for agriculture (Wei et al., 2006). However, due to their special structure and low water retention properties, natural or engineering problems such as landslides, unstable rock formations, and droughts often occur in red bed soil areas (Sun & Kong, 2011; Y. Wang et al., 2017; L. Yan et al., 2016; P. Yan et al., 2021; Z. T. Zhang et al., 2020). Knowledge of the unsaturated hydraulic properties of purple soils is important for understanding and predicting these hazards (Iverson, 2000; H. L. Wang et al., 2015; Wu et al., 2018; Zhao et al., 2015). However, there are a limited number of unsaturated hydraulic data of purple soils available, while no systematic analyses of unsaturated hydraulic properties have ever been reported. The lack of reliable unsaturated hydraulic data significantly restricts accurate hazard predictions related to purple soils.

Typically, the constitutive soil hydraulic properties include the soil water retention function relating the water content ( $\theta$ ) with the pressure head ( $h$ ) and the hydraulic conductivity ( $K$ ) as a function of  $\theta$  or  $h$ . Many laboratory methods have been developed over the years to determine the hydraulic properties of soils (Dane & Hopmans, 2002; Novák & Hlaváčikova, 2019). Among these, column outflow and evaporation methods have been used widely to simultaneously obtain pressure head and unsaturated conductivity data (e.g., Hopmans et al., 2002; Kool et al., 1985; Wendroth et al., 1993; Zhuang et al., 2017). Early versions of the evaporation method usually involved measurements of the evaporation rate and the pressure head at multiple depths of the sample (Šimůnek et al., 1998; Wendroth et al., 1993; and references therein). A new popular semiautomated evaporation setup is the HYPROP system of the METER Group, which was designed to continuously collect tensiometer readings at two depths from the evaporating surface as well as corresponding sample weights during the entire evaporation process (Peters et al., 2015; Schindler et al., 2010). The HYPROP system has been used recently to obtain unsaturated hydraulic data of a range of soils and rocks (e.g., Coelho et al., 2017; Lipovetsky et al., 2020; Schindler, 2014; Shokrana & Ghane, 2020).

### Core Ideas

- Hydraulic properties of Chinese subtropical purple soils (Regosols and Entisols) were measured experimentally.
- The data were analyzed in terms of unimodal and bimodal unsaturated soil hydraulic functions.
- Bimodal porosity was not found to be overly significant for most samples.
- Pedotransfer functions closely matched the slope of the water retention curves, except near saturation.

As noted above, a comprehensive and precise understanding of unsaturated hydraulic properties is essential for many evaluations related to purple soils. However, to the best of our knowledge, there are few experimental unsaturated hydraulic data in current literature covering the full moisture range. The aim of this study is to offer a systematic experimental analysis of the unsaturated hydraulic properties of purple soils. For this purpose, we collected six soil samples from Nanxiong Basin, a typical red bed area in southern China (P. Yan et al., 2021). The hydraulic properties were measured over the full moisture range by combining HYPROP evaporation data obtained at relatively wet and intermediate moisture contents with psychrometer dew point (WP4C) measurements at relatively dry conditions. The data were analyzed in terms of unimodal and bimodal unsaturated soil hydraulic models and also compared also predictions obtained using pedotransfer functions.

## 2 | MATERIALS AND METHODS

### 2.1 | Materials

The purple soils were collected from Nanxiong Basin (Figure 1), located in Shaoguan City, northern Guangdong Province, China, between coordinates of 114° 29' 50'' to 114° 33' 30'' E and 25° 13' 23'' to 25° 16' 57'' N. Nanxiong Basin is a typical red bed area in southern China.

The soil samples, denoted as PS1 through PS6, were collected in situ from the surface horizons of six sites in Nanxiong Basin. Microscope images (Sigma 300) of the samples are presented in Figure 2. The purple soil particles typically exhibited a relatively rounded morphology, with rough and uneven surfaces. The mineral composition (X'Pert PRO MPD, Nalytical) of a typical purple soil is shown in Table 1. Table 2 provides an overview of selected properties of the soil samples, which were determined mostly after the HYPROP measurements. Soil organic matter was measured by oxidation with potassium dichromate ( $K_2Cr_2O_7$ ).

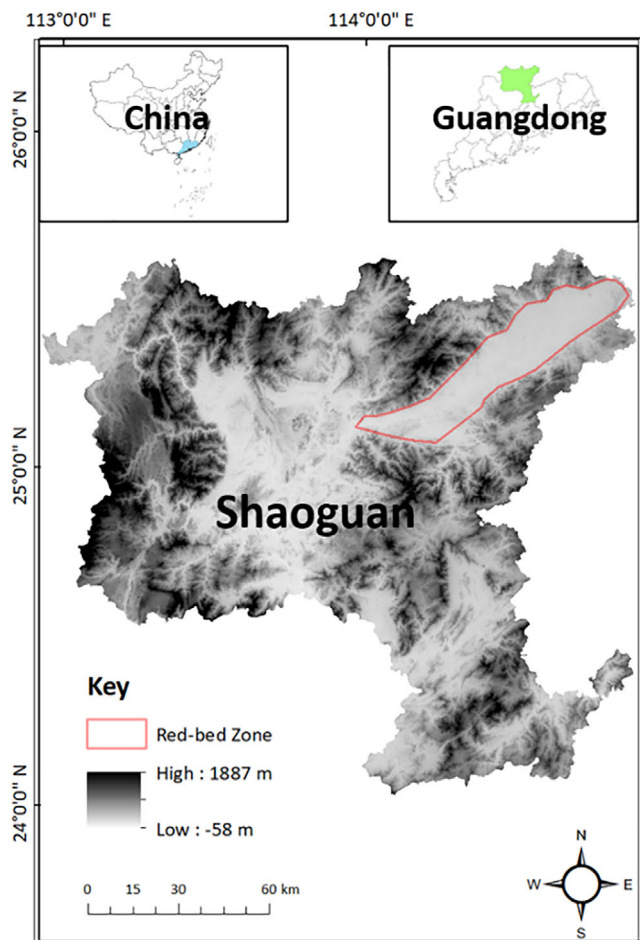


**FIGURE 1** Map of Nanxiang Basin in Shaoguan City, Northern Guangdong Province, China.

Saturated hydraulic conductivities were determined using the constant-head method (Reynolds et al., 2002), yielding values within the range of 24–82 cm/day.

## 2.2 | Experimental procedures

We determined hydraulic properties of the soil samples using a combination of the evaporation (HYPROP) and the psychrometry (WP4C) methods. For the HYPROP measurements in the intermediate and relatively wet region, we used the standard setup as described in the operational manual by METER (2015). The collected samples were first saturated overnight, ensuring the soil surface gleamed with water to confirm their complete saturation. The saturated samples subsequently were mounted directly onto the sensor unit. Two tensiometers of different lengths were inserted from below into the 5-cm soil columns. While the upper surface of the soil samples was exposed to air for evaporation, the entire setup (including sensor unit and soil sample) was positioned on a mass balance to record evaporation rate data. Subse-

quently, we derived water content and hydraulic conductivity directly or inversely from the sample weight and the pressure heads (Peters et al., 2015). Following the experiments, the soil samples were oven-dried to obtain corrected dry weights.

The HYPROP system was used to obtain hydraulic data exclusively in the relatively wet range (i.e., for  $pF < 3$ , where  $pF$  is defined as  $\log_{10} |h|$  with  $h$  representing the pressure head in cm). This limitation stems from the bubble entry properties of the tensiometers. The WP4C dew point method (METER) was subsequently used to obtain water retention data in the relatively dry region. WP4C psychrometers measure the sum of matric and osmotic (negligible) potentials during equilibration of liquid-phase water and vapor-phase water in a sealed container (Bittelli & Flury, 2009; Solone et al., 2012). The dimensions of the WP4C sample container were 1 cm in height and 4 cm in diameter. When packing the saturated soil samples into the container, we ensured that the porosities matched those used for the HYPROP system. The upper surface of the initially saturated WP4C samples was exposed to evaporation, thus creating primary drying conditions similar to those of the HYPROP measurements. Pressure heads of the samples were measured every 15 min, while water contents were determined gravimetrically until negligible changes in the sample weights were observed. The WP4C measurements were deemed reliable within the approximate range of  $pF = 4.0$  ( $-10^4$  cm pressure head) to  $pF = 6.5$  (about  $-3.1 \times 10^4$  cm pressure head) (METER, 2021). All experiments were conducted under constant temperature and humidity conditions, employing degassed deionized water to saturate the soil samples.

## 2.3 | Soil hydraulic models

The van Genuchten (VG) model (van Genuchten, 1980) and several other VG type models were used for analyses of the data. The standard VG soil hydraulic property expressions are given as follows:

$$S_e(h) = \frac{\theta(h) - \theta_r}{\theta_s - \theta_r} = \frac{1}{[1 + |\alpha h|^n]^m} \quad (1)$$

$$K(S_e) = K_s S_e^l \left[ 1 - (1 - S_e^{1/m})^m \right]^2 \quad (2)$$

where  $\theta$  is the volumetric water content,  $\theta_s$  and  $\theta_r$  denote saturated and residual water contents, respectively,  $S_e$  is effective water saturation,  $h$  is the soil water pressure head,  $K$  is the hydraulic conductivity (here given as a function of  $S_e$ ),  $K_s$  is the saturated hydraulic conductivity, and  $\alpha$ ,  $n$ ,  $m$  ( $m = 1 - 1/n$ ), and  $l$  are quasi-empirical shape parameters.

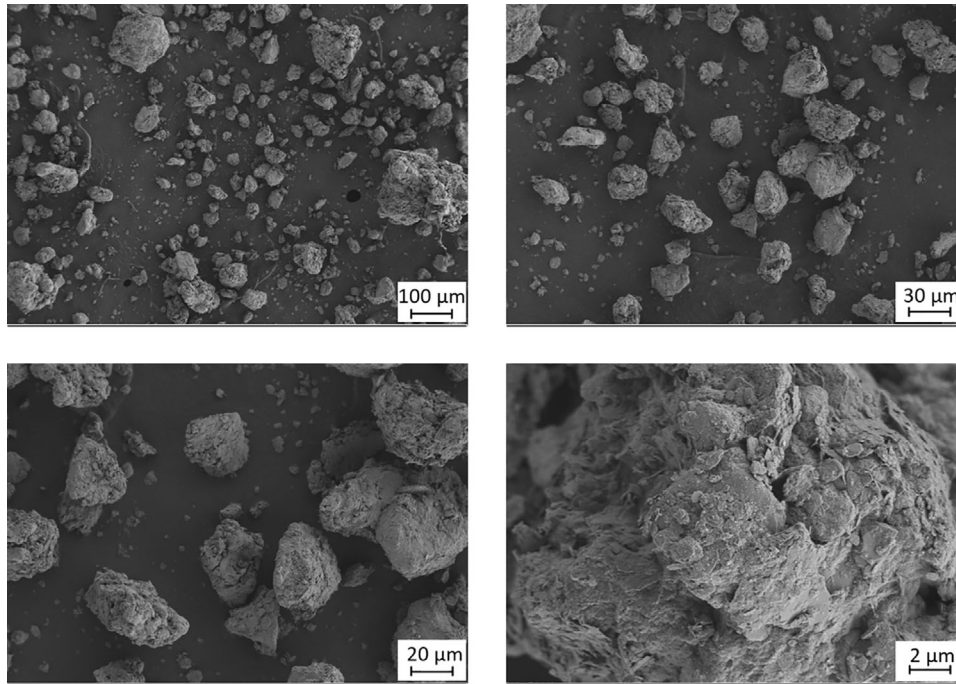


FIGURE 2 Microscope images of the purple soil samples.

TABLE 1 Mineral composition of a typical purple soil.

Quartz	K-feldspar	Albite	Pyrite	Illite/montmorillonite	Illite	Kaolinite	Chlorite
78.4	0.50	3.00	1.30	4.75	5.16	5.65	1.24

Note: Total mineralogical composition in mass %.

TABLE 2 Soil physical properties of the six purple soils used in this study.

	PS1	PS2	PS3	PS4	PS5	PS6
Soil organic matter (g/kg)	22.24 ± 2.35					
Mean particle diameter, $d_{50}$ (mm)	0.45	0.57	0.52	0.55	0.59	0.60
Uniformity coefficient, $C_u$ ( $d_{60}/d_{10}$ )	5.27	3.78	4.13	4.19	3.79	4.25
Saturated hydraulic conductivity, $K_s$ (cm/day)	82.0	24.0	82.0	75.0	55.0	53.0
Porosity (-)	0.51	0.44	0.47	0.48	0.45	0.47
Bulk density ( $\text{g}/\text{cm}^3$ )	1.30	1.48	1.40	1.38	1.46	1.40
Sand (%)	76.7	75.7	72.8	71.4	80.9	78.8
Silt (%)	10.0	5.5	15.5	16.8	1.0	4.3
Clay (%)	13.3	18.8	11.7	11.8	18.1	16.9

The above VG functions represent a unimodal-type hydraulic model that mainly considers capillary flow. To capture the possible bimodal nature of the purple soils, dual-porosity VG type models were also employed. For the bimodal functions, we used the water retention formulation initially

proposed by Durner (1994) and later extended by Priesack and Durner (2006) to the hydraulic conductivity:

$$S_e(h) = \frac{\theta(h) - \theta_r}{\theta_s - \theta_r} = \frac{w_1}{[1 + |\alpha_1 h|^{n_1}]^{m_1}} + \frac{w_2}{[1 + |\alpha_2 h|^{n_2}]^{m_2}} \quad (3)$$

$$K(S_e) = K_s \frac{(w_1 S_1 + w_2 S_2)^l \left\{ w_1 \alpha_1 \left[ 1 - (1 - S_e^{1/m_1})^{m_1} \right] + w_2 \alpha_2 \left[ 1 - (1 - S_e^{1/m_2})^{m_2} \right] \right\}^2}{(w_1 \alpha_1 + w_2 \alpha_2)^2} \quad (4)$$

where  $w_i$  ( $i = 1, 2$ ) represents weight factors attributed to the macropore and micropore regions, respectively (with  $w_1 + w_2 = 1$ ), and  $\alpha_i$ ,  $n_i$ , and  $m_i$  ( $i = 1, 2$ ) are shape parameters for the bimodal model, with  $m_i = 1 - 1/n_i$ .

To account for film, corner, and vapor flow at the lower water content levels, we extended the unimodal and bimodal VG models to a broader pressure head range by incorporating the van Genuchten–Peters–Durner–Iden (VGPDI) formulation (Iden & Durner, 2008; Peters & Durner, 2008; Peters et al., 2015). In the VGPDI model, an additional fitting parameter,  $pF_{dry}$ , is to be optimized based on the experimental measurements. Optimizations were conducted using the HYPROP-FIT software (METER, 2015; Pertassek et al., 2015). Several statistical parameters, notably the root mean square error (RMSE) and the Akaike information criterion (AICc), were used to evaluate the models. Their respective equations are given by:

$$RMSE = \sqrt{\sum_{i=1}^{n_t} \frac{1}{n_t} (y_i^c - y_i)^2} \quad (5)$$

$$AICc = \frac{2k - 2L}{n_t} + \left[ \frac{2k(k+1)}{n_t - k - 1} \right] \quad (6)$$

where  $n_t$  is the number of measurements;  $y_i$  and  $y_i^c$  are the measured and fitted values, respectively;  $k$  denotes the number of fitting parameters in the model, and  $L$  is the logarithmic likelihood. The Akaike information criterion with a correction (AICc) is typically negative, with larger absolute values indicating a superior fit of the model.

### 3 | RESULTS AND DISCUSSION

Figure 3 shows the observed HYPROP and WP4C water retention data of the six purple soil samples. The HYPROP measurements covered water contents up to  $pF = 3$ , while the WP4C measurements contributed data at the drier range. The measured data were fitted using four different models: the original VG model, the bimodal van Genuchten (BiVG) model, the VGPDI model, and the bimodal van Genuchten–Peters–Durner–Iden (BiVGPDI) model. Values of the saturated water content were held constant as individually

measured data for all optimizations. The resulting parameter values and statistical analyses are presented in the [Supporting Information](#).

The measured and fitted retention curves for PS1 are shown in Figure 3a. Except for some minor oscillations in the water retention data near saturation, the observed retention data were quite uniform, with no discernible evidence of showing bimodality. The optimized water retention curves yielded nearly identical results within the wet moisture range, while showing only minor differences in the relatively dry range, particularly when using the VG and BiVG models. The VGPDI and BiVGPDI models exhibited significant overlap and good agreement with the water retention data. The resulting fitting parameters and accuracy analysis are included in Table S1. The parameter  $RMSE_\theta$  in the table is the root mean square error values for water content and AICc is the Akaike information criterion. As anticipated, the BiVGPDI model, with its greater number of fitting parameters, predicted the observations best among the four models. However, it is noteworthy that the VGPDI model, despite its fewer fitting parameters, also described the data very well.

The measurements for sample PS2 did not exhibit distinct bimodal patterns (see Figure 3b). Regarding the water retention optimizations, the VG function showed some discrepancies with the measurements, while the BiVG results displayed a slightly more bimodal shape than what appears to be evident in the data. The VGPDI and BiVGPDI models both closely matched the measurements. Based on the accuracy analysis in Table S2, the BiVGPDI model again showed the best fit with the data, with the VGPDI model also performing well, albeit with minimally larger deviations with the data. One caution is needed about the BiVGPDI fit. This function showed a bimodal shape between HYPROP and WP4C data, where few data were present. It is likely caused by considerable uncertainty in the macropore side of the bimodal functional description. This suggests that overparameterization may be an issue in this case.

The water retention data of PS3 exhibited a more distinct bimodal pattern (see Figure 3c). Regarding the fittings, discrepancies are apparent between the VG model and the measured data. The BiVG model described the water retention data much better. The VGPDI and BiVGPDI models both showed notable enhanced agreement with the measure data although they did not fully capture the bimodal characteristic (see Table S3).

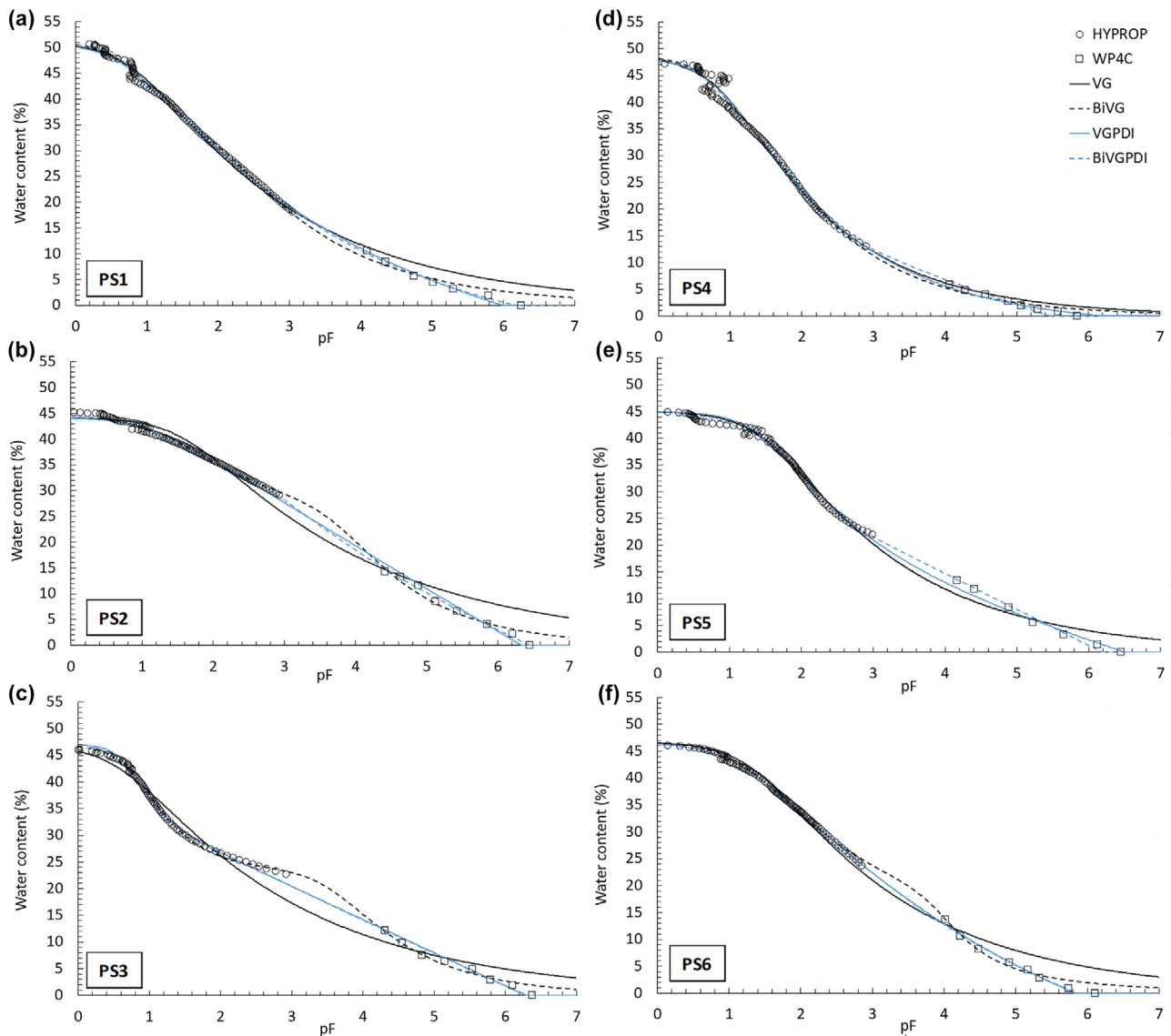


**FIGURE 3** Measured and fitted water retention curves of purple soils using various hydraulic models. BiVG, bimodal van Genuchten; BiVGPD, bimodal van Genuchten-Peters–Durner–Iden; VG, van Genuchten; VGPD, van Genuchten-Peters–Durner–Iden.

The measured data for the purple soil PS4 were quite uniform (Figure 3d). The optimized water retention curves of the four models exhibited close agreement with each other as well as with the data. This is also reflected by the values of  $RMSE_{\theta}$  in Table S4. For soil PS5, the water retention data and fitted curves did not display any discernible bimodal characteristics, except for some drastic oscillations in the water retention data near saturation (see Figure 3e). All of the models described the data well, except perhaps the standard VG formulation, which showed some deviations in the very dry moisture range. As expected, the VGPD model performed better in that part of the retention curve. Detailed information of the fitted and statistical parameter values for PS5 are provided in Table S5.

Regarding purple soil sample RS6 (Figure 3f), the water retention data exhibited only a very minimal nonuniform trend. Within the wet moisture range, the VG model described

the data very well, but encountered limitations in the dry moisture range. The BiVG model gave better agreement with the data, which had a remarkable bimodal nature. Nevertheless, the results obtained using the VGPD and BiVGPD models were nearly indistinguishable, both offering commendable predictive accuracy for the data. The statistical analysis and the fitting parameter values are listed in Table S6.

Of all six samples, only sample PS3 exhibited a distinct bimodal trend in the observed water retention data over the full moisture range. In terms of model fittings, the BiVGPD model was capable of reproducing all of the observed data very well. This could be attributed to having more fitting parameters compared to the other models. Nevertheless, it is important to note that for many of the purple soil samples, the results obtained using the BiVGPD model exhibited

**TABLE 3** Experiments (Exp.) and pedotransfer function (PTF) predicted hydraulic parameters of the six purple soils.

Parameter (unit)	PS1		PS2		PS3		PS4		PS5		PS6	
	Exp.	PTF										
$\alpha$ (1/cm)	0.141	0.030	0.025	0.026	0.246	0.031	0.124	0.030	0.030	0.025	0.044	0.026
$n$ (-)	1.20	1.56	1.17	1.51	1.18	1.53	1.29	1.51	1.23	1.64	1.21	1.61
$\theta_r$ (-)	0.00	0.06	0.00	0.06	0.00	0.05	0.00	0.05	0.00	0.07	0.00	0.07
$\theta_s$ (-)	0.51	0.45	0.44	0.41	0.47	0.42	0.48	0.42	0.45	0.42	0.47	0.43
$K_s$ (cm/day)	82.0	123.0	24.0	53.7	82.0	79.3	75.0	78.3	55.0	83.5	53.0	92.1

considerable overlap with those generated by the VGPD model. This overlap suggests that the bimodal nature of the purple soils may not be of significance. Furthermore, the good agreement of the models with the PDI formations (VGPD and BiVGPD models) implies that corner and film flow mechanisms are dominant, especially under relative dry conditions. The rough and uneven surfaces of purple soil grains have the potential to significantly enhance water retention (Di Raimo et al., 2022).

The results were further compared with predicted VG parameters values using soil pedotransfer functions. We used for this purpose the Rosetta light pedotransfer functions (Schaap & Leij, 1998a, 1998b; Schaap et al., 1998) as embedded with the RETC and HYDRUS software packages (Šimůnek et al., 2016). Rosetta predictions were based on the measured fractions of sand, silt, and clay, and the bulk density. The predicted hydraulic parameters are shown in Table 3. The calculated  $\alpha$  values exhibited slight variations around 0.030 1/cm. These values closely matched the fitted values based on the measurements only for three soil samples, with the exception of soils PS1, PS3, and PS4. The predicted  $n$  values were slightly larger than the fitted values, resulting in relatively steeper retention curves. The predicted hydraulic conductivities were fairly close to the measured values only for PS3 and PS4. The Rosetta pedotransfer functions primarily estimates soil hydraulic properties based on sand, clay, and silt fractions. They do not consider information regarding macropores and pore connectivity, which are mostly evident near the air entry pressure (related to the  $\alpha$  value in the VG model) and in the saturated conductivity. Therefore, it is reasonable to expect less accurate predictions of  $\alpha$  and  $K_s$ . In general, however, the hydraulic parameter values estimated with the pedotransfer model closely matched the slope of water retention curves of the purple soils, with the exception of water contents near the air entry value and the saturated conductivity.

## 4 | SUMMARY AND CONCLUSIONS

In this study, we measured the hydraulic properties of six purple soils covering the full moisture range. Observed water retention data were fitted using unimodal and BiVG type

models. Bimodal behavior was not found to be extensive for most of the soil samples. The BiVGPD model with its more numerous fitting parameters yielded the best agreement with the observations. Nevertheless, the results obtained using the BiVGPD model were very similar to those produced by the VGPD model for most of the soil samples. The good agreement of the PDI models suggests that film and corner flow may be significant under dry moisture conditions. Predictions with the Rosetta pedotransfer model were found to reasonably match the slope of water retention curves, although discrepancies were observed for the saturated conductivity and the  $\alpha$  parameter.

This work has provided comprehensive analyses of the unsaturated hydraulic properties of purple soils over the entire moisture range. The obtained hydraulic parameter values could be used for agriculture and engineering management applications, including risk analyses. It is important to note that our study involved a limited number of purple soil samples. Investigations for a more diverse set of purple soils from around the world are clearly needed. Additionally, the development of more appropriate pedotransfer models is imperative, particularly for enhancing predictions of the saturated conductivity and air entry (or  $\alpha^{-1}$ ) values specific to purple soils.

## AUTHOR CONTRIBUTIONS

**Luwen Zhuang:** Funding acquisition; investigation; methodology; writing—original draft. **Hao Chen:** Investigation; writing—original draft. **Ping Yan:** Resources. **Xingmei Liang:** Investigation. **Wenceslau G. Teixeira:** Methodology. **Martinus Th. van Genuchten:** Methodology; writing—review and editing. **Kairong Lin:** Funding acquisition; project administration; writing—review and editing.

## ACKNOWLEDGMENTS

The authors acknowledge financial support by Projects of the National Key R&D Program of China (2022YFC3002903) and the National Natural Science Foundation of China (Grant Nos. 42377057 and 42007165).

## ORCID

Luwen Zhuang  <https://orcid.org/0000-0002-6300-9999>

Wenceslau G. Teixeira  <https://orcid.org/0000-0002-2010-6078>

Martinus Th. van Genuchten  <https://orcid.org/0000-0003-1654-8858>

Kairong Lin  <https://orcid.org/0000-0001-6533-3357>

## REFERENCES

- Bittelli, M., & Flury, M. (2009). Errors in water retention curves determined with pressure plates. *Soil Science Society of America Journal*, 73(5), 1453–1460. <https://doi.org/10.2136/sssaj2008.0082>
- Coelho, C. R., Zhuang, L., Barbosa, M., Soto, M. A., & van Genuchten, M. Th. (2017). Further tests of the HYPROP evaporation method for estimating the unsaturated soil hydraulic properties. *Journal of Hydrology and Hydromechanics*, 66, <https://doi.org/10.1515/johh-2017-0046>
- Dane, J. H., & Hopmans, J. W. (2002). Water retention and storage: Laboratory. In J. H. Dane & G. C. Topp (Eds.), *Methods of soil analysis: Part 4—Physical methods* (pp. 675–720). SSSA. <https://doi.org/10.2136/sssabookser5.4.c25>
- Di Raimo, L. A. D. L., Couto, E. G., Demattê, J. A. M., Amorim, R. S. S., Torres, G. N., Cremon, C., de Mello, D. C., Bocuti, E. D., Poppiel, R. R., da Silva, A. N., Lima, L. N., & Neto, L. C. G. (2022). Sand fractions micromorphometry detected by Vis-NIR-MIR and its impact on water retention. *European Journal of Soil Science*, 73(2), e13227.
- Durner, W. (1994). Hydraulic conductivity estimation for soils with heterogeneous pore structure. *Water Resources Research*, 30(2), 211–223. <https://doi.org/10.1029/93WR02676>
- FAO. (1988). *Soil map of the world* (World Soil Resources Report 60). FAO.
- He, Y. (2003). *Purple soils in China* (2). Chinese Science Press.
- Hopmans, J. W., Šimůnek, J., Romano, N., & Durner, W. (2002). Inverse modeling of transient water flow. In J. H. Dane & G. C. Topp (Eds.), *Methods of soil analysis: Part 4—Physical methods* (pp. 963–1008). SSSA.
- Iden, S. C., & Durner, W. (2008). Free-form estimation of soil hydraulic properties using Wind's method. *European Journal of Soil Science*, 59, 1228–1240. <https://doi.org/10.1111/j.1365-2389.2008.01068.x>
- Iverson, R. M. (2000). Landslide triggering by rain infiltration. *Water Resources Research*, 36(7), 1897–1910. <https://doi.org/10.1029/2000WR900090>
- Kool, J. B., Parker, J. C., & van Genuchten, M. Th. (1985). Determining soil hydraulic properties from onestep outflow experiments by parameter estimation. I. Theory and numerical studies. *Soil Science Society of America Journal*, 49(6), 1348–1354. <https://doi.org/10.2136/sssaj1985.03615995004900060004x>
- Lipovetsky, T., Zhuang, L., Teixeira, W. G., Boyd, A., Pontedeiro, E. M., Moriconi, L., & van Genuchten, M. Th. (2020). HYPROP measurements of the unsaturated hydraulic properties of a carbonate rock sample. *Journal of Hydrology*, 591, 125706. <https://doi.org/10.1016/j.jhydrol.2020.125706>
- Meng, Q., Li, S., Liu, B., Hu, J., Liu, J., Chen, Y., & Ci, E. (2023). Appraisal of soil taxonomy and the world reference base for soil resources applied to classify purple soils from the eastern Sichuan basin, China. *Agronomy*, 13, 1837. <https://doi.org/10.3390/agronomy13071837>
- METER. (2015). *Operation manual HYPROP 2*. METER Group AG.
- METER. (2021). *WP4C manual*. METER Group AG.
- Novák, V., & Hlaváčikova, H. (2019). *Applied soil hydrology*. Springer. [https://doi.org/10.1007/978-3-030-01806-1\\_7](https://doi.org/10.1007/978-3-030-01806-1_7)
- Pertassek, T., Peters, A., & Durner, W. (2015). *HYPROP-FIT software user's manual, V.3.0*. UMS GmbH.
- Peters, A., & Durner, W. (2008). A simple model for describing hydraulic conductivity in unsaturated porous media accounting for film and capillary flow. *Water Resources Research*, 44(11). <https://doi.org/10.1029/2008wr007136>
- Peters, A., Iden, S. C., & Durner, W. (2015). Revisiting the simplified evaporation method: Identification of hydraulic functions considering vapor, film and corner flow. *Journal of Hydrology*, 527, 531–542. <https://doi.org/10.1016/j.jhydrol.2015.05.020>
- Priesack, E., & Durner, W. (2006). Closed-form expression for the multi-modal unsaturated conductivity function. *Vadose Zone Journal*, 5(1), 121–124. <https://doi.org/10.2136/vzj2005.0066>
- Reynolds, W. D., Elrick, D. E., Youngs, E. G., Amoozegar, A., Booltink, H. W. G., & Bouma, J. (2002). Saturated and field-saturated water flow parameters. In J. H. Dane & G. C. Topp (Eds.), *Methods of soil analysis. Part 4. physical methods* (pp. 797–801). SSSA. <https://doi.org/10.2136/sssabookser5.4.c30>
- Schaap, M. G., & Leij, F. J. (1998a). Using neural networks to predict soil water retention and soil hydraulic conductivity. *Soil and Tillage Research*, 47(1–2), 37–42. [https://doi.org/10.1016/S0167-1987\(98\)00070-1](https://doi.org/10.1016/S0167-1987(98)00070-1)
- Schaap, M. G., & Leij, F. J. (1998b). Database-related accuracy and uncertainty of pedotransfer functions. *Soil Science*, 163(10), 765–779.
- Schaap, M. G., Leij, F. J., & van Genuchten, M. Th. (1998). Neural network analysis for hierarchical prediction of soil hydraulic properties. *Soil Science Society of America Journal*, 62(4), 847–855. <https://doi.org/10.2136/sssaj1998.03615995006200040001x>
- Schindler, U. (2014). A novel method for quantifying soil hydraulic properties. In L. Mueller, A. Saparov, & G. Lischeid (Eds.), *Novel measurement and assessment tools for monitoring and management of land and water resources in agricultural landscapes of Central Asia* (pp. 145–158). Springer International Publishing. [https://doi.org/10.1007/978-3-319-01017-5\\_7](https://doi.org/10.1007/978-3-319-01017-5_7)
- Schindler, U., Durner, W., von Unold, G., & Muller, L. (2010). Evaporation method for measuring unsaturated hydraulic properties of soils: Extending the measurement range. *Soil Science Society of America Journal*, 74(4), 1071–1083. <https://doi.org/10.2136/sssaj2008.0358>
- Shokrana, M. S. B., & Ghane, E. (2020). Measurement of soil water characteristic curve using HYPROP2. *MethodsX*, 7, 100840. <https://doi.org/10.1016/j.mex.2020.100840>
- Šimůnek, J., van Genuchten, M. Th., & Šejna, M. (2016). Recent developments and applications of the HYDRUS computer software packages. *Vadose Zone Journal*, 15, 1–25. <https://doi.org/10.2136/vzj2016.04.0033>
- Šimůnek, J., Wendroth, O., & van Genuchten, M. Th. (1998). Parameter estimation analysis of the evaporation method for determining soil hydraulic properties. *Soil Science Society of America Journal*, 62, 894–905. <https://doi.org/10.2136/sssaj1998.03615995006200040007x>
- Solone, R., Bittelli, M., Tomei, F., & Morari, F. (2012). Errors in water retention curves determined with pressure plates: Effects on the soil water balance. *Journal of Hydrology*, 470–471, 65–74. <https://doi.org/10.1016/j.jhydrol.2012.08.017>
- Soil Survey Staff. (2022). *Keys to soil taxonomy* (13th ed.). USDA-Natural Resources Conservation Service.

- Sun, F., & Kong, J. M. (2011). Research on the cusp-catastrophic of the stability of the red beds landslide in western Yunnan. *Advanced Materials Research*, 261–263, 1645–1649. <https://doi.org/10.4028/www.scientific.net/AMR.261-263.1645>
- Turner, P. (1978). Red beds. In R. W. Fairbridge & Bourgeois (Eds.), *Encyclopedia of Sedimentology* (pp. 905–909). Springer. [https://doi.org/10.1007/3-540-31079-7\\_167](https://doi.org/10.1007/3-540-31079-7_167)
- van Genuchten, M. Th. (1980). A closed-form equation for predicting the hydraulic conductivity of unsaturated soils. *Soil Science Society of America Journal*, 44(5), 892–898. <https://doi.org/10.2136/sssaj1980.03615995004400050002x>
- Wang, H. L., Tang, X. Y., Zhang, W., Song, S. B., & McKenzie, B. M. (2015). Within-year changes in hydraulic properties of a shallow Entisol in farmland and forestland. *Vadose Zone Journal*, 14(7), 1–15. <https://doi.org/10.2136/vzj2014.11.0163>
- Wang, Y., Liu, J., Yan, S., Yu, L., & Yin, K. (2017). Estimation of probability distribution of shear strength of slip zone soils in middle jurassic red beds in Wanzhou of China. *Landslides*, 14, 2165–2174. <https://doi.org/10.1007/s10346-017-0890-z>
- Wei, C., Ni, J., Gao, M., Xie, D., & Hasegawa, S. (2006). Anthropogenic pedogenesis of purple rock fragments in Sichuan Basin, China. *Catena*, 68, 51–58. <https://doi.org/10.1016/j.catena.2006.04.022>
- Wendroth, O., Ehlers, W., Hopmans, J. W., Klage, H., Halbertsma, J., & Wösten, J. H. M. (1993). Reevaluation of the evaporation method for determining hydraulic functions in unsaturated soils. *Soil Science Society of America Journal*, 57, 1436–1443. <https://doi.org/10.2136/sssaj1993.03615995005700060007x>
- Wu, L. Z., Zhang, L. M., Zhou, Y., Xu, Q., Yu, B., Liu, G. G., & Bai, L. Y. (2018). Theoretical analysis and model test for rainfall-induced shallow landslides in the red-bed area of Sichuan. *Bulletin of Engineering Geology and the Environment*, 77(4), 1343–1353. <https://doi.org/10.1007/s10064-017-1126-0>
- Yan, L., Liu, P., Peng, H., Milica, K.-G., & Lin, K. (2019). Laboratory study of the effect of temperature difference on the disintegration of redbed softrock. *Physical Geography*, 40(2), 149–163. <https://doi.org/10.1080/02723646.2018.1559418>
- Yan, L., Peng, H., Hu, Z., Milica, K.-G., Vladimir, G., Chen, Z., & Scott, S. (2016). Stone pillar rockfall in Danxia landform area, Mt. Langshan, Hunan Province, China. *Physical Geography*, 37(5), 327–343. <https://doi.org/10.1080/02723646.2016.1218244>
- Yan, L. B., & Milica, K. G. (2019). Land degradation and management of red beds in China: Two case studies. *Journal of Mountain Science*, 16(11), 2591–2604. <https://doi.org/10.1007/s11629-019-5560-2>
- Yan, P., Lin, K., Wang, Y., Zheng, Y., Gao, X., Tu, X., & Bai, C. (2021). Spatial interpolation of red bed soil moisture in Nanxiong basin, South China. *Journal of Contaminant Hydrology*, 242(2021), 103860. <https://doi.org/10.1016/j.jconhyd.2021.103860>
- Zhang, X. C., Liu, G., & Zheng, F. L. (2017). A simple enrichment correction factor for improving erosion estimation by rare earth oxide tracers. *Vadose Zone Journal*, 16(12), 1–10. <https://doi.org/10.2136/vzj2017.03.0068>
- Zhang, Z. T., Gao, W. H., Zeng, C. F., Tang, X. Y., & Wu, J. Y. (2020). Evolution of the disintegration breakage of red-bed soft rock using a logistic regression model. *Transportation Geotechnics*, 24, 100382. <https://doi.org/10.1016/j.tgeo.2020.100382>
- Zhao, Q. H., Li, D. Q., Zhuo, M. N., Guo, T. L., Liao, Y. S., & Xie, Z. Y. (2015). Effects of rainfall intensity and slope gradient on erosion characteristics of the red soil slope. *Stochastic Environmental Research and Risk Assessment*, 29(2), 609–621. <https://doi.org/10.1007/s00477-014-0896-1>
- Zhong, S., Han, Z., Du, J., Ci, E., Ni, J., Xie, D., & Wei, C. (2019). Relationships between the lithology of purple rocks and the pedogenesis of purple soils in the Sichuan Basin, China. *Scientific Reports*, 9, Article 13272. <https://doi.org/10.1038/s41598-019-49687-9>
- Zhou, C. Y., Yang, X., Liang, Y. H., Du, Z. C., Liu, Z., Huang, W., & Ming, W. H. (2019). Classification of red-bed rock mass structures and slope failure modes in South China. *Geosciences*, 9(6), 273. <https://doi.org/10.3390/geosciences9060273>
- Zhuang, L., Bezerra Coelho, C. R., Hassanizadeh, S. M., & van Genuchten, M. Th. (2017). Analysis of the hysteretic hydraulic properties of unsaturated soil. *Vadose Zone Journal*, 16(5), 1–9. <https://doi.org/10.2136/vzj2016.11.0115>

## SUPPORTING INFORMATION

Additional supporting information can be found online in the Supporting Information section at the end of this article.

**How to cite this article:** Zhuang, L., Chen, H., Yan, P., Liang, X., Teixeira, W. G., van Genuchten, M. Th., & Lin, K. (2024). Unsaturated hydraulic property measurements of subtropical anthropogenic (purple) soils in China. *Vadose Zone Journal*, 23, e20334. <https://doi.org/10.1002/vzj2.20334>